

# Water Conservation & Management (WCM)

DOI: http://doi.org/10.26480/wcm.01.2025.178.183



ISSN: 2523-5664 (Print) ISSN: 2523-5672 (Online) CODEN: WCMABD

RESEARCH ARTICLE

# MODELING AND OPTIMIZATION OF THREE-DIMENSIONAL Y-SHAPED MICRO-MIXERS FOR BEST MICROFLUIDIC MIXING EFFICIENCY

Z. El Mouden\*, A. Taouallah, S. Mordane, B. Ifegous, K. Abderrafi, R. Adhiri

Hassan II University of Casablanca, Laboratory of Engineering and Materials (LIMAT), Faculty of Science Ben M'Sick, Casablanca Morocco

\* Corresponding Author Email: elmouden.za@gmail.com

This is an open access journal distributed under the Creative Commons Attribution License CC BY 4.0, which permits unrestricted use, distribution, and reproduction in any medium, provided the original work is properly cited

## ARTICLE DETAILS

#### Article History:

Received 23 November 2024 Revised 18 December 2024 Accepted 03 February 2025 Available online 15 March 2025

## **ABSTRACT**

Microfluidic devices are essential in applications requiring precise fluid control, particularly in biotechnology and medicine, where efficient mixing at the microscale is critical. The control of flows in this type of device becomes increasingly difficult; the flows are highly laminar, which significantly reduces the performance of the mixing. It is then necessary to imagine innovative designs to improve it. This study aims to evaluate the performance of a passive 3D Y-shaped serpentine micromixer using Computational Fluid Dynamics (CFD). The primary objective is to optimize mixing by taking advantage of transverse flows and chaotic advection of moving fluids. Water and ethanol are utilized as test fluids to analyze the influence of viscosity and flow rates on mixing efficiency. Simulations reveal that the 3D serpentine design significantly enhances mixing at moderate flow rates, optimizing the interaction between advection and diffusion processes. Ethanol, due to its higher viscosity, exhibits extended interaction times and better mixing efficiency compared to water. These findings underscore the critical role of geometric design and fluid properties in enhancing mixing performance. The study provides valuable insights for developing high-efficiency micromixers, paving the way for advanced lab-on-chip systems requiring precise and reliable fluid handling.

# KEYWORDS

Numerical simulation, Computational Fluid Dynamics CFD, passive Micromixer, lab-on-chip, serpentine channel, pressure drop, flow rate, laminar flow, Water and Ethanol.

# 1. Introduction

Microfluidics has emerged as a thriving field of study over the past few years, with a wide range of applications that contribute to its vitality. It can be defined as the study of fluid flows in channels, capillaries, or porous media with dimensions of a few micrometers or less (Zeng et al., 2011). This area of research is particularly recognized for its significant potential in biotechnological and medical fields, including DNA chips and lab-on-a-chip systems (Downs et al., 2023; Sharma and Sharma, 2022).

Microfluidic devices and lab-on-a-chip systems offer advantages such as reduced reactant consumption, improved control over reaction variables (such as reactant concentration and temperature), and the ability to control spatial parameters (Li et al., 2022). As a result, they are now widely utilized in chemical and biological sciences for various applications, from the synthesis of nanoparticle and colloidal systems to medical diagnostics(Chiu et al., 2017) (Illath et al., 2022). Additionally, they play a crucial role in cell biology, facilitating tasks such as chemical reactions (Cheng et al., 2020), the synthesis or sequencing of nucleic acids (Su et al., 2021) , and DNA purification (Chen et al., 2007).

Almost every use of these devices in chemical analysis and manufacture or biological assays/bioengineering necessitates the capacity to mix two or more chemical or biological components effectively and reliably. Thus, the mixing of fluids is a fundamental and crucial process in the development of microfluidic systems. It is also one of the most challenging features to achieve since the fluid flow is laminar, with low Reynolds numbers on the

order of 0.1 to 0.01 in a typical water-based microfluidic system (Buchegger et al., 2011). In such conditions, mixing primarily occurs through diffusion, making it a much slower process compared to turbulent mixing techniques commonly used in larger-scale systems.

Various methods for enhancing mixing in microfluidic devices have been proposed, which can be categorized into active or passive mixers. Active mixers require an external energy source, such as mechanical ultrasonic transducers thermal actuators, periodic electro-osmotic flow generators, magnetic field, and dielectrophoretic transducers (Lan and Yang, 2024; Lv and Chen, 2022; Douroum et al., 2021; Lim et al., 2010; Zhou et al., 2021). The implementation of active mixing in microfluidics often necessitates additional equipment, complex manufacturing processes, causing heat generation, and high power consumption. As result there is increasing interest in developing passive mixers as an alternative.

In contrast, passive mixers do not require external actuators; instead, they rely on the kinetic energy and hydrodynamic behavior of the moving fluids (Douroum et al., 2022). The mixing performance can be enhanced by increasing the chaotic mechanism between the mixing components, this can be achieved through the use of 2D channels or more complex 3D configurations. Several geometric designs have been proposed to improve mixing efficiency, including microchannels with serpentine elements, T-micromixer with helical elements (Mahammedi et al., 2023), two-layered crossing channels, and microchannels featuring grooves or obstacles on the bottom walls (Karthikeyan and Sujatha, 2018; Ritter et al., 2016a; Ottino, 1989; Cai et al., 2017; Karthikeyan and Sujatha, 2018; Hossain et al., 2017)

**Quick Response Code** 

Access this article online



Website: www.watconman.org DOI:

10.26480/wcm.01.2025.178.183

Karthikeyan et al. designed a Y-shaped microfluidic mixer featuring both rectangular and triangular obstacles to effectively mix fluids with very low diffusivity. Remarkably, they achieved a 100% mixing efficiency at a flow rate corresponding to a Reynolds number (Re) of 25 (Karthikeyan et al., 2017). Ortega-Casanova et al. demonstrated that three-dimensional micromixers can induce chaotic mixing, resulting in significant increase in the mixing efficiency (Ortega-Casanova and Lai, 2018). Mahammedi et al. Investigated T-micromixer with helical elements at different angles (0°, 30°, 45°, 60°, and 90°) using CFD analysis. The results showed that the 90° angle configuration produced the best mixing performance (Mahammedi et al., 2023). Arockiam et al. developed a 3D serpentine micromixer with bends, and their computational fluid dynamics (CFD) predictions indicated that the number of 90-degree bends in the device is a key factor influencing mixing efficiency, rather than the length of the straight sections (Arockiam et al., 2021).

In this work, a 3D microfluidic design is proposed to enhance the mixing efficiency of two fluids; we introduce a passive micromixer that induces transversal flows extending the interface between the fluids and thereby increasing the efficiency of diffusional mixing. As a result, Computational fluid dynamic (CFD) is used to investigate the effect of the proposed configuration, inlet flow rate and the diffusion coefficient of fluids towards mixing efficiency.

# 2. MATERIALS AND METHODS

#### 2.1 Geometry And Description

The design of the microfluidic device proposed in this study is illustrated in Figure 1. The device exhibits a rectangular cross-section and incorporates two inlet channels, each channel measures  $1600~\mu m$  in length,  $100~\mu m$  in width, and  $50~\mu m$  in depth. These inlet channels serve as the entry points for the fluids being investigated, specifically water and ethanol.

The core element of the microfluidic device is the mixing channel, which consists of eight serpentine units. This channel is responsible for promoting fluid mixing and enhancing contact between the two fluid streams. The mixing channel is 3500  $\mu m$  long and maintains the same width and depth dimensions as the inlet channels.

Figure 1 provides a visual representation of the microfluidic device's design, offering a clear overview of its key components and dimensions.



Figure 1: Geometry of the microfluidic mixer

Fluids are introduced into the device through two separate inlet channels, and they merge within the primary microchannel. During this study, we aim to simulate the mixing of these two fluids at different flow rates, ranging from  $0.1~\mu\text{l/min}$ ,  $0.5~\mu\text{l/min}$ ,  $1~\mu\text{l/min}$ , to  $2~\mu\text{l/min}$ .

## 2.2 Numerical modelling

The fluid flow through the micromixer is modeled using the Navier-Stokes model for incompressible fluids, which describes the flow of viscous fluids with momentum balances for each component of the momentum vector in all spatial dimensions under the assumption that the fluid's density and viscosity are constant.

The Navier-Stokes model that describes the incompressible fluid flow is given by the following equations:

$$\rho \frac{\partial \theta}{\partial t} = -\rho(\theta, \nabla)\theta - \nabla p + \eta \nabla^2 \theta \tag{1}$$

$$\nabla \cdot \vartheta = 0 \tag{2}$$

Where,  $\vartheta$  (m·s<sup>-1</sup>) is the velocity vector,  $\rho$  (kg·m<sup>-3</sup>) is the fluid density,  $\eta$  (kg·m<sup>-1</sup>·s<sup>-1</sup>) is the fluid viscosity, t (s) is the time, and p (Pa) is the pressure.

The concentration field inside the microchannel can be represented by the convection diffusion equation to calculate the distribution of the concentration  $c \, (\text{mol} \cdot \text{m}^{-3})$  through the mixer, which is expressed as:

$$\frac{\partial c}{\partial t} = D\nabla^2 c - \vartheta \cdot \nabla c \tag{3}$$

In the above equation, D ( $m^2 \cdot s^{-1}$ ) and c ( $mol \cdot m^{-3}$ ) are the diffusion constant and the concentration of the species, respectively. The boundary conditions employed in the study were as follows: no slip at channel walls, equal volume flow rate at each inlet, zero pressure at the outlet, molar concentration of  $0.516 \, mol \cdot m^{-3}$  at one inlet, and molar concentration of  $0 \, mol \cdot m^{-3}$  at the other inlet. These boundary conditions were selected to facilitate the study of fluid mixing and concentration distribution within the microfluidic device.

To investigate the degree of mixing, the mixing index of the species at any given cross-section in the mixing channel is calculated by using Eqs. (4) and (5) as follows (Okuducu and Aral, 2019a):

$$\sigma = \sqrt{\frac{1}{N} \sum_{i=1}^{N} (C_i - C_m)^2} \tag{4}$$

$$MI = 1 - \sqrt{\frac{\sigma^2}{\sigma_{max}^2}} \tag{5}$$

Where,  $\sigma$  is the standard deviation of the mole fraction concentration, N is the total number of sampling points across the channel's cross-section, C\_i denotes the normalized concentration of the fluid at each cross-section of the device, and C\_m denotes the average concentration of the fluid at the inlets. According to Eq. (5), the mixing efficiency, M = 0%, represents the species' entirely unmixed state, whereas M = 100% represents the species' completely mixed condition. A mixing efficiency of roughly 80-100% is adequate for mixing applications (Karthikeyan et al., 2017), (Ortega-Casanova and Lai, 2018), (Kuo and Jiang, 2014).

## 3. RESULTS

#### 3.1 Mesh Independence

Mesh independence in computational study refers to the notion of guaranteeing that the resolution of the computational mesh used in the simulation has no substantial effect on the results of a numerical simulation (Okuducu and Aral, 2018) (Okuducu and Aral, 2019b). To verify the mesh independence of a study, a frequent method is to simulate with different mesh sizes ranging from coarse to fine. The results are then compared, and the simulation is considered mesh-independent if the difference between them is negligible as the mesh is refined. When a simulation exhibits mesh independence, it indicates that results are reliable and accurate, and that the choice of mesh size or type does not heavily influence them. For this reason, a mesh-independence investigation was initially performed to investigate the mixing efficiency at various units for three different mesh configurations, i.e., Fine (102.876), extremely fine (7.342.997), and a defined mesh (26.380.673). Therefore, water is chosen as the input fluid for both the inlets of the micromixer with different concentrations. The properties of the input fluid are given as follows: Density is 998 kg·m<sup>-3</sup>, Viscosity is 10<sup>-3</sup> kg·m<sup>-1</sup>·s<sup>-1</sup>, and the diffusion constant is set to  $2.1 \times 10^{-10} \text{ m}^2 \cdot \text{s}^{-1}$ . The flow rate of the fluid in both the inlets is considered the same (0.5  $\mu$ l/min), and the fluid concentrations (c) are taken as 0 mol·m<sup>-3</sup> for the upper inlet and 0.516 mol·m<sup>-3</sup> for the lower inlet. The table below summarizes different parameters for each mesh configuration.

Table 1: Mesh configuration		
Mesh	Number of cells	Element size
Fine	102.876	24.9
Extremely fine	7342997	6.1
Defined mesh	26.380.673	4

Figure 2 shows the evolution of the concentration profiles along the micromixer for the three mesh configurations at a flow rate of  $0.5~\mu l/min$ . Dark blue in the picture represents the concentration of  $0~mol/m^3$ , whereas dark red denotes the concentration of  $0.516~mol/m^3$ . As we can see, the concentration profile in the micromixer has changed color to green, suggesting that the mixing of fluids has occurred and that the concentration has approached the value of  $0.256~mol/m^3$ , the average concentration at the outlet of the mixer. However, we can observe that the mixing unit differs from one mesh configuration to another.

The graph in Figure 3 represents mixing efficiency at various units of the mixer. It shows that the extremely fine and defined mesh configurations are identical, indicating a consistent level of results. As the fine mesh is refined, its results converge towards those of the extremely fine mesh,

making any differences negligible. Therefore, we can conclude that mesh independence has been achieved, particularly with the use of finer and extremely fine meshes (Khosravi Parsa et al., 2014). Consequently, the

extreme mesh was selected to ensure the accuracy, reliability, and credibility of the numerical results.

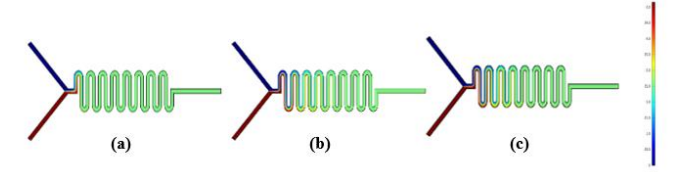


Figure 2: Concentration distribution along the micromixer at  $Qv = 0.5 \mu l/min$  for: (a): fine mesh, (b): extremely fine mesh, (c): defined mesh

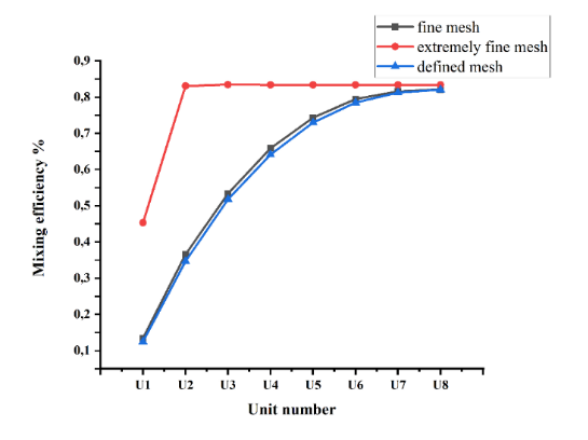


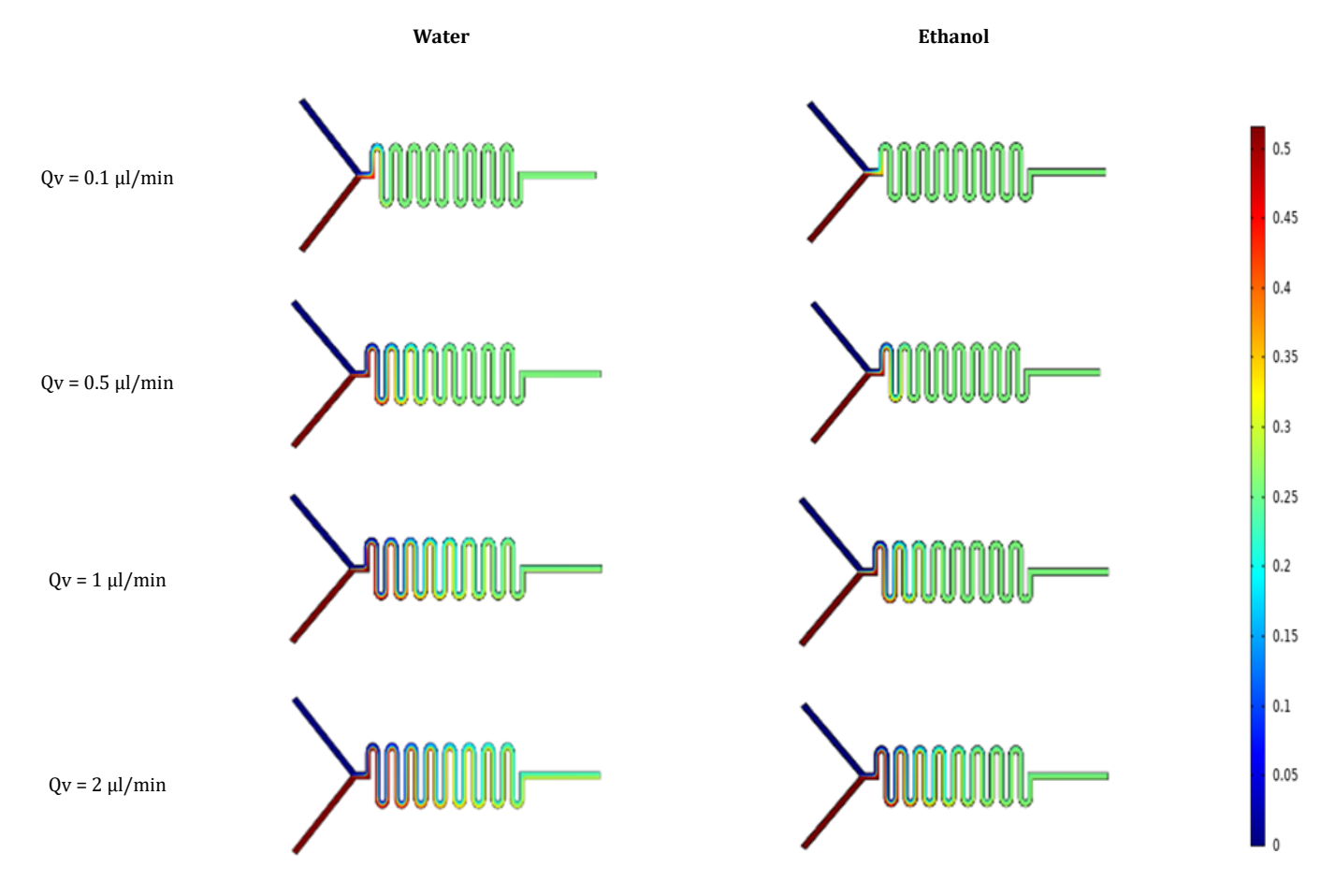
Figure 3: Mixing Efficiency at different units of the micromixer at  $Qv = 0.5\mu l/min$  for different mesh configurations

### 3.2 Water and Ethanol

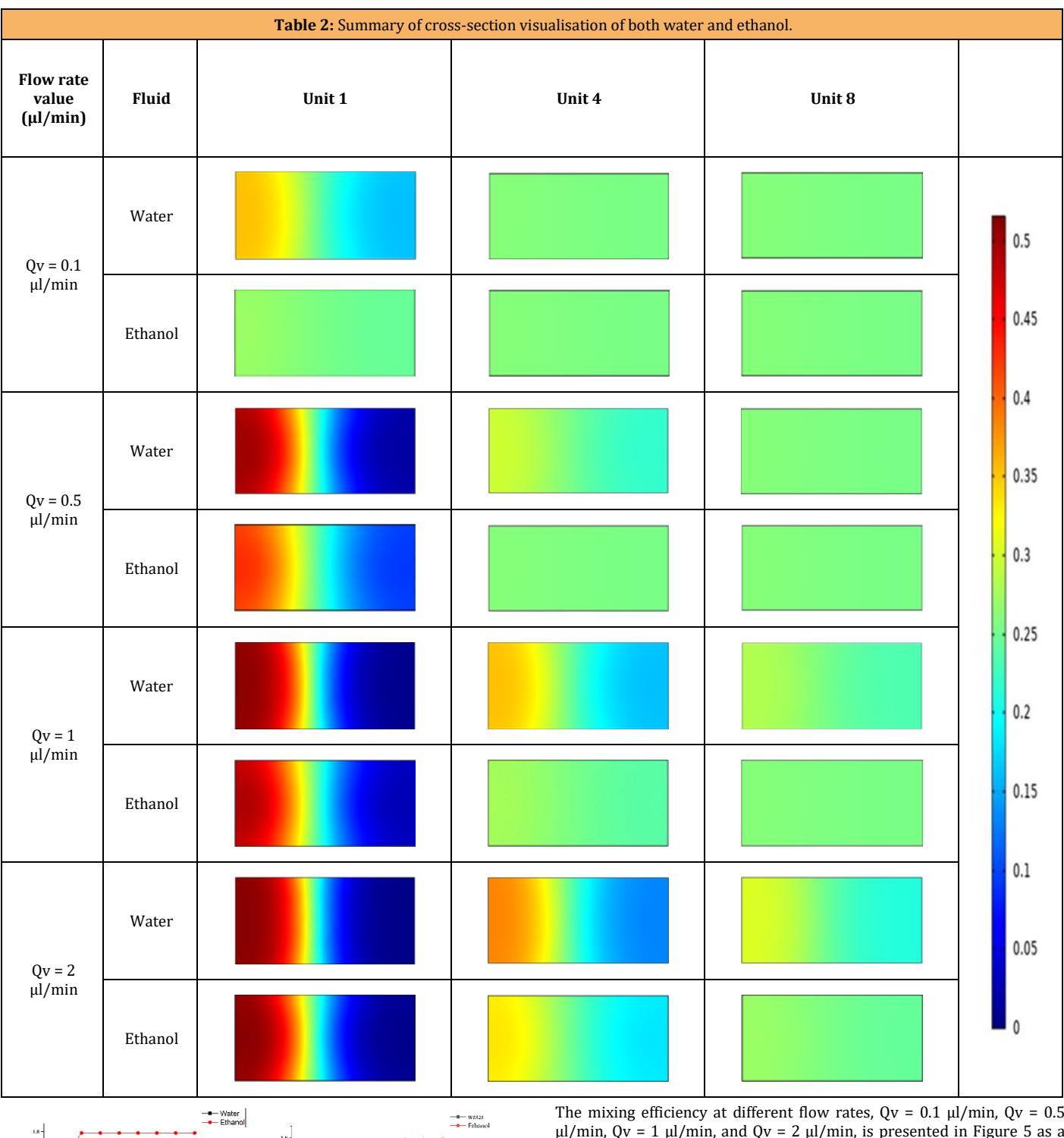
The comparison of water with ethanol involves using the same volumetric flow rates at two inlets of the micromixer, considering their different densities and viscosities. Water has a density ( $\rho$ ) of 998 kg/m³ and a viscosity ( $\mu$ ) of  $10^{-3}$  kg·m⁻¹·s⁻¹, while ethanol has a density of 789 kg/m³ and a viscosity of  $1.2\times10^{-3}$  kg·m⁻¹·s⁻¹ (Ahmad Termizi et al., 2020). These values correspond to the properties of the substances at a temperature of  $20^{\circ}C$ 

Figure 4 illustrates the simulated concentration results for water and ethanol at various flow rates. In the figure, dark blue represents a concentration of 0 mol/m³, while dark red indicates a concentration of 0.516 mol/m³. When the color shifts to green across all flow rate values, it suggests that the concentration has stabilized at 0.256 mol/m³, which is the average concentration at the mixer's outlet, signifying complete mixing of the samples.

Table 2 presents a summary of the cross-sectional visualization for both water and ethanol at different flow rates in Unit 1, Unit 4, and Unit 8. It is evident that the cross-sectional color for water across all three units is more intense than that for ethanol



**Figure 4:** Concentration distribution along the micromixer for different flow rate values for both water and ethanol



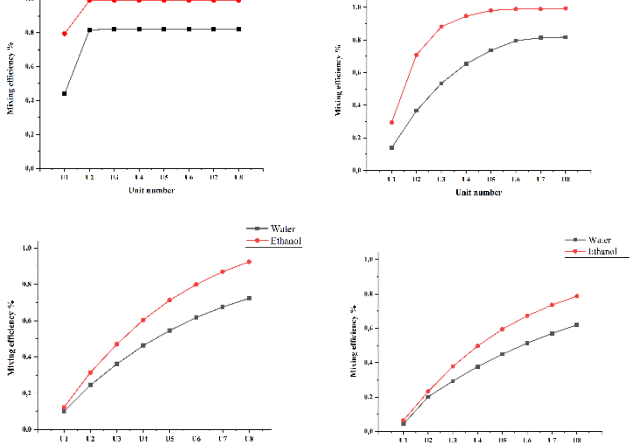


Figure 5: Mixing Efficiency at different units of the micromixer for water and ethanol for different Qv

The mixing efficiency at different flow rates,  $Qv = 0.1 \mu l/min$ , Qv = 0.5 $\mu$ l/min, Qv = 1  $\mu$ l/min, and Qv = 2  $\mu$ l/min, is presented in Figure 5 as a function of the channel's distance (reported as unit number) for both water and ethanol.

## 3.2.1 Pressure Drop

Pressure drop is defined as the difference in total pressure between two points of a fluid-carrying network. A pressure drop occurs when frictional forces, caused by the resistance to flow, act on a fluid as it moves through the channel. The key factors that determine resistance to fluid flow are the fluid's velocity as it travels through the pipe and its viscosity.

A pressure drop is therefore expressed in Pascal ( $\Delta P$ ) according to the following formula

$$\Delta P = \frac{v_1^2}{2}\rho + P_1 - \frac{v_2^2}{2}\rho - P_2 \tag{5}$$

Where v denotes the velocity, P is the pressure, and  $\rho$  is the fluid density.

The following graph presents a comparison of pressure drop for both water and ethanol at different flow rates.

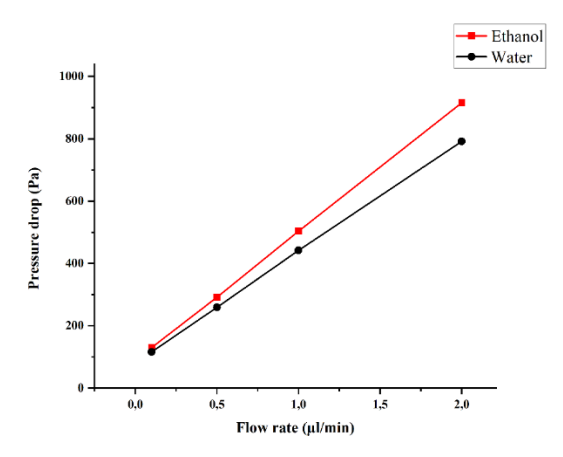


Figure 6: Pressure drop for water and ethanol at different flow rates.

The graph in figure 6 reveals a clear relationship between flow rate and pressure drop: as the flow rate increases, the pressure drop also increases, and conversely, as the flow rate decreases, the pressure drop diminishes. This variation in pressure drop shows a linear trend throughout the mixing length. It's important to note that the pressure drop required for mixing ethanol is significantly higher than that needed for mixing water. As the flow rate rises, there is a corresponding decline in mixing efficiency and an increase in pressure drop. The design of the serpentine mixer was specifically designed to maximize mixing efficiency while minimizing the pressure drop associated with energy consumption (Viktorov and Nimafar, 2013).

#### 4. DISCUSSIONS

Previously, many studies have been conducted on serpentine micromixer, however there has been a notable lack on evaluating 3D simulation of these mixers. Existing studies has focused on high flow rate usually on the order of 1mL/min or more which does not reflect the low flow rates typically observed in microfluidic systems (Alijani et al., 2019; Khosravi Parsa et al., 2014). In the present work, a detailed 3D study of a micromixer at a very low flow rate of 0.1  $\mu L/min$  is addressed to analyze fluid dynamics within the serpentine micromixer.

CFD simulation was carried out to examine the effect of flow rate and the fluid's viscosity on the mixing performance. From Figure 4 and Table 2, we can see that the concentration distribution varies significantly, particularly for ethanol. Mixing occurs rapidly in the initial units of the main channel. This can be attributed to the fact that ethanol is slightly more viscous than water; as a result, its flow is slower, leading to a longer residence time for ethanol mixtures compared to water (Orsi et al., 2013).

It can be seen in Figure 5 that significant mixing was achieved in the serpentine channel immediately after the first unit for both water and ethanol. This can be explained by the fact that at low flow rates, there is no turbulence or secondary flows responsible on enhancing mixing. Instead, mixing depends primarily on molecular diffusion (Mariotti et al., 2022). The efficiency of this mixing is further influenced by the residence time of each fluid. Since ethanol has a higher viscosity than water, resulting in a slower flow, the mixing efficiency for ethanol is greater than that for water, reaching 100% at the beginning of the channel specifically at the second unit of the serpentine mixer.

However, as Qv increases, chaotic advection becomes the dominant transport mechanism, and the effect of molecular diffusion becomes significantly less important. This process occurs at higher flow rates or when specific designs are introduced; such as the serpentine micromixer. At this stage, the reduced residence time limits the opportunity for molecular diffusion, leading to a drop in mixing efficiency; which can reach up to 80% and 60%, respectively, for ethanol and water at the device outlet.

# 5. CONCLUSION

The study focuses on fluid dynamics and mixing efficiency in a three-dimensional Y-shaped microfluidic mixer, comparing water and ethanol. The results indicate that as the flow rate decreases, mixing efficiency improves, particularly in the initial sections of the mixer. Numerical simulations demonstrate that ethanol consistently achieves a higher mixing index than water. At a flow rate of  $Qv=0.1\,\mu l/min$ , ethanol reaches

a 100% mixing index, while water achieves only 80%.

Additionally, the study highlights a significant difference in the pressure drop required for mixing ethanol compared to water. Future research should investigate energy-efficient designs and conduct experimental validation under real-world conditions. Extending the analysis to other fluids and scaling the system for industrial applications could enhance its applicability. Emphasizing sustainability and integrating the findings into biomedical or diagnostic platforms would further increase the impact of these insights.

#### REFERENCES

- Ahmad Termizi, S.N.A., Khor, C.Y., Nawi, M.A.M., Ahmad, N., Ishak, M.I., Rosli, M.U., Jamalludin, M.R., 2020. Computational Fluid Dynamics (CFD) Simulation on Mixing in T-Shaped Micromixer. IOP Conf. Ser. Mater. Sci. Eng. 932, 012006. https://doi.org/10.1088/1757-899X/932/1/012006
- Alijani, H., Özbey, A., Karimzadehkhouei, M., Koşar, A., 2019. Inertial Micromixing in Curved Serpentine Micromixers with Different Curve Angles. Fluids 4, 204. https://doi.org/10.3390/fluids4040204
- Arockiam, S., Cheng, Y.H., Armenante, P.M., Basuray, S., 2021. Experimental determination and computational prediction of the mixing efficiency of a simple, continuous, serpentine-channel microdevice. Chem. Eng. Res. Des. 167, Pp. 303–317.
- Buchegger, W., Wagner, C., Lendl, B., Kraft, M., Vellekoop, M.J., 2011. A highly uniform lamination micromixer with wedge shaped inlet channels for time resolved infrared spectroscopy. Microfluid. Nanofluidics 10, Pp. 889–897. https://doi.org/10.1007 /s10404-010-0722-0
- Cai, G., Xue, L., Zhang, H., Lin, J., 2017. A review on micromixers. Micromachines 8, Pp. 274.
- Chen, X., Cui, D., Liu, C., Li, H., Chen, J., 2007. Continuous flow microfluidic device for cell separation, cell lysis and DNA purification. Anal. Chim. Acta 584, Pp. 237–243. https://doi.org/10.1016/j.aca.2006.11.057
- Cheng, Y.H., Barpaga, D., Soltis, J.A., Shutthanandan, V., Kargupta, R., Han, K.S., McGrail, B.P., Motkuri, R.K., Basuray, S., Chatterjee, S., 2020. Metal-organic framework-based microfluidic impedance sensor platform for ultrasensitive detection of perfluorooctanesulfonate. ACS Appl. Mater. Interfaces 12, Pp. 10503–10514.
- Chiu, D.T., Demello, A.J., Di Carlo, D., Doyle, P.S., Hansen, C., Maceiczyk, R.M., Wootton, R.C., 2017. Small but perfectly formed? Successes, challenges, and opportunities for microfluidics in the chemical and biological sciences. Chem 2, Pp. 201–223.
- Douroum, E., Kouadri, A., Tahiri, A., Brihmat, M., Khelladi, S., 2022. Hydrodynamic and Kinematic Study to Analyze the Mixing Efficiency of Short Passive Micromixers. Ind. Eng. Chem. Res. 61, Pp. 5994–6009. https://doi.org/10.1021/acs.iecr.2c00084
- Douroum, E., Laouedj, S., Kouadri, A., Naas, T.T., Khelladi, S., Benazza, A., 2021. High hydrodynamic and thermal mixing performances of efficient chaotic micromixers: A comparative study. Chem. Eng. Process.-Process Intensif. 164, 108394.
- Downs, B.M., Hoang, T.-M., Cope, L., 2023. Increasing the Capture Rate of Circulating Tumor DNA in Unaltered Plasma Using Passive Microfluidic Mixer Flow Cells. Langmuir 39, Pp. 3225–3234. https://doi.org/10.1021/acs.langmuir.2c02919
- Hossain, S., Lee, I., Kim, S.M., Kim, K.-Y., 2017. A micromixer with two-layer serpentine crossing channels having excellent mixing performance at low Reynolds numbers. Chem. Eng. J. 327, Pp. 268–277.
- Illath, K., Kar, S., Gupta, P., Shinde, A., Wankhar, S., Tseng, F.-G., Lim, K.-T., Nagai, M., Santra, T.S., 2022. Microfluidic nanomaterials: From synthesis to biomedical applications. Biomaterials 280, Pp. 121247.
- Karthikeyan, K., Sujatha, L., 2018. Study of permissible flow rate and mixing efficiency of the micromixer devices. Int. J. Chem. React. Eng. 17, 20180047.
- Karthikeyan, K., Sujatha, L., Sudharsan, N.M., 2017. Numerical modeling and parametric optimization of micromixer for low diffusivity fluids. Int. J. Chem. React. Eng. 16, 20160231.
- Khosravi Parsa, M., Hormozi, F., Jafari, D., 2014. Mixing enhancement in a passive micromixer with convergent-divergent sinusoidal microchannels and different ratio of amplitude to wave length.

- Comput. Fluids 105, Pp. 82–90. https://doi.org/10.1016/j.compfluid. 2014.09.024
- Kuo, J.-N., Jiang, L.-R., 2014. Design optimization of micromixer with square-wave microchannel on compact disk microfluidic platform. Microsyst. Technol. 20, Pp. 91–99.
- Lan, M., Yang, F., 2024. Applications of dielectrophoresis in microfluidicbased exosome separation and detection. Chem. Eng. J. 152067.
- Li, Z., Zhang, B., Dang, D., Yang, X., Yang, W., Liang, W., 2022. A review of microfluidic-based mixing methods. Sens. Actuators Phys. 344, 113757. https://doi.org/10.1016/j.sna. 2022.113757
- Lim, C.Y., Lam, Y.C., Yang, C., 2010. Mixing enhancement in microfluidic channel with a constriction under periodic electro-osmotic flow. Biomicrofluidics 4.
- Lv, H., Chen, X., 2022. Novel Study on the Mixing Mechanism of Active Micromixers Based on Surface Acoustic Waves. Ind. Eng. Chem. Res. 61, 10264–10274. https://doi.org/10.1021/acs.iecr.2c01539
- Mahammedi, A., Tayeb, N.T., Rahmani, K., Al-Kassir, A., Cuerda-Correa, E.M., 2023. Exploring the Bioenergy Potential of Microfluidics: The Case of a T-Micromixer with Helical Elements for Sustainable Energy Solutions. Energies 16, 7123. https://doi. Org/10.339 0/en16207123
- Mariotti, A., Galletti, C., Brunazzi, E., Salvetti, M.V., 2022. Mixing sensitivity to the inclination of the lateral walls in a T-mixer. Chem. Eng. Process.

  Process Intensif. 170, 108699. https://doi.org/10.1016/j.cep.2021.108699
- Okuducu, M.B., Aral, M.M., 2018. Performance analysis and numerical evaluation of mixing in 3-D T-shape passive micromixers. Micromachines 9, Pp. 210.
- Okuducu, M.B., Aral, M.M., 2019a. Novel 3-d t-shaped passive micromixer design with helicoidal flows. Processes 7, Pp. 637.

- Okuducu, M.B., Aral, M.M., 2019b. Computational evaluation of mixing performance in 3-d swirl-generating passive micromixers. Processes 7. Pp. 121.
- Orsi, G., Roudgar, M., Brunazzi, E., Galletti, C., Mauri, R., 2013. Waterethanol mixing in T-shaped microdevices. Chem. Eng. Sci. 95, Pp. 174–183. https://doi.org/10.1016/j.ces.2013.03.015
- Ortega-Casanova, J., Lai, C.-H., 2018. CFD study about the effect of using multiple inlets on the efficiency of a micromixer. Assessment of the optimal inlet configuration working as a microreactor. Chem. Eng. Process.-Process Intensif. 125, Pp. 163–172.
- Ottino, J.M., 1989. The Kinematics of Mixing: Stretching, Chaos, and Transport. Cambridge University Press.
- Ritter, P., Osorio-Nesme, A., Delgado, A., 2016. 3D numerical simulations of passive mixing in a microchannel with nozzle-diffuser-like obstacles. Int. J. Heat Mass Transf. 101, Pp. 1075–1085.
- Sharma, B., Sharma, A., 2022. Microfluidics: Recent Advances Toward Labon-Chip Applications in Bioanalysis. Adv. Eng. Mater. 24, 2100738. https://doi.org/10.1002/adem. 202100738
- Su, W., Liang, D., Tan, M., 2021. Nucleic acid-based detection for foodborne virus utilizing microfluidic systems. Trends Food Sci. Technol. 113, Pp. 97–109.
- Viktorov, V., Nimafar, M., 2013. A novel generation of 3D SAR-based passive micromixer: efficient mixing and low pressure drop at a low Reynolds number. J. Micromechanics Microengineering 23, 055023.
- Zeng, S., Liu, X., Xie, H., Lin, B., 2011. Basic Technologies for Droplet Microfluidics, in: Lin, B. (Ed.), Microfluidics, Topics in Current Chemistry. Springer Berlin Heidelberg, Berlin, Heidelberg, Pp. 69–90. https://doi.org/10.1007/128\_2011\_149
- Zhou, R., Surendran, A., Wang, J., 2021. Fabrication and characteristic study on mixing enhancement of a magnetofluidic mixer. Sens. Actuators Phys. 326, 112733. https://doi.org/10.1016/j.sna.2021.112733

